Journal of Applied Polymer Science

Investigations of Environmental Stress Cracking Resistance of HDPE/EVA and LDPE/EVA Blends

Yang Chen
The State Key Lab of Polymer Materials Engineering, Polymer Research Institute of Sichuan University, Chengdu 610065, China
Correspondence to: Y. Chen (E-mail: cy3262276@163.com)

ABSTRACT: HDPE/poly(ethylene-*co*-vinylacetate) (EVA) and low-density polyethylene (LDPE)/EVA blends were tested and compared with respect to their environmental stress cracking resistance (ESCR) using the Bell-telephone test. The time to failure in the ESCR test improves with increasing EVA content, and considerable improvements were produced for LDPE/EVA blends while small improvements were observed for HDPE/EVA blends. Thermal, rheological, mechanical, and morphological studies were conducted which established a quantitative relationship between morphological features and composition. Furthermore, the failed specimens were further characterized by scanning electron microscopy and fractographic methodology to investigate the failure mechanism for ESCR samples. © 2013 Wiley Periodicals, Inc. J. Appl. Polym. Sci. **2014**, *131*, 39880.

KEYWORDS: phase behavior; structure–property relations; polyolefins

Received 28 May 2013; accepted 22 August 2013
DOI: 10.1002/app.39880

INTRODUCTION

Polyethylene (PE), as one of the most widely used general plastics with good flow properties, has drawn much attention of both industrial engineers and academic researchers. It is widely used in outdoor applications in which dielectric, mechanical, and thermal behaviors combined with high environmental stress cracking resistance (ESCR) are a matter of major concern.[1] Ethylene copolymers such as poly(ethylene-*co*-vinylacetate) (EVA) are produced by free-radical polymerization in a bulk process, such as that used for low-density polyethylene (LDPE) production, involving high pressures and temperatures.[2,3] PE/EVA blends are widely used in many applications such as shrinkable films, multilayer packaging, and wire and cable coating.[4–6] Addition of EVA onto different grades of PE improves their toughness, transparency, ESCR, and the capacity of the filler carrying.[7] As a result, blends of EVA with LDPE or high-density polyethylene (HDPE) would be expected to yield an improvement in ESCR.

Semicrystalline polymers such as PE often show brittle fracture under stress if exposed to stress cracking agents. In such polymers, the crystallites are connected by the tie molecules through the amorphous phase. The tie molecules play a decisive role in the mechanical properties of the polymer, through the transmission of load. Stress cracking agents act to lower the cohesive forces which maintain the tie molecules in the crystallites, thus facilitating their "pull-out" and disentanglement from the lamellae. Consequently, cracking is initiated at stress values lower than the critical stress level of the material. In general, the failure process begins with the embrittlement of the polymer. Then the crack initiation takes place, which is favored by the acting load. Environmental stress cracking (ESC) type of failure is characterized by the presence of macroscopic cracks and a fibrillar structure of the craze, formed ahead of the crack.[8]

The modifying effect of the EVA on the ESCR of LDPE has been reported by Borisova and Kressler,[6] and they found that EVA species considerably improved the ESCR of LDPE because the EVA particles can stop crack propagation. But up to now no information has been reported on the ESCR behavior of LDPE/EVA and HDPE/EVA systems from a comparative viewpoint. Morphological examinations clearly revealed a phase-separated morphology for both systems in which the droplet size of LDPE/EVA system is smaller than that of HDPE/EVA attributed to lower interfacial tension.[9] Since the fracture behaviors of the blends are influenced by the blend morphology as well as interfacial interaction between phases, consideration of morphologies of different blends should be useful.[10] To better understand such phenomenon, we present the results below regarding the behavior of PE blends. The systems studied were HDPE/EVA and LDPE/EVA blends, in which the composition ratio is systematically varied.

EXPERMENTAL

Materials and Sample Preparation

Materials. The materials used in this study were HDPE, LDPE, and EVA with a melt index of 7.2 g/10 min, 1.8 g/10 min, and

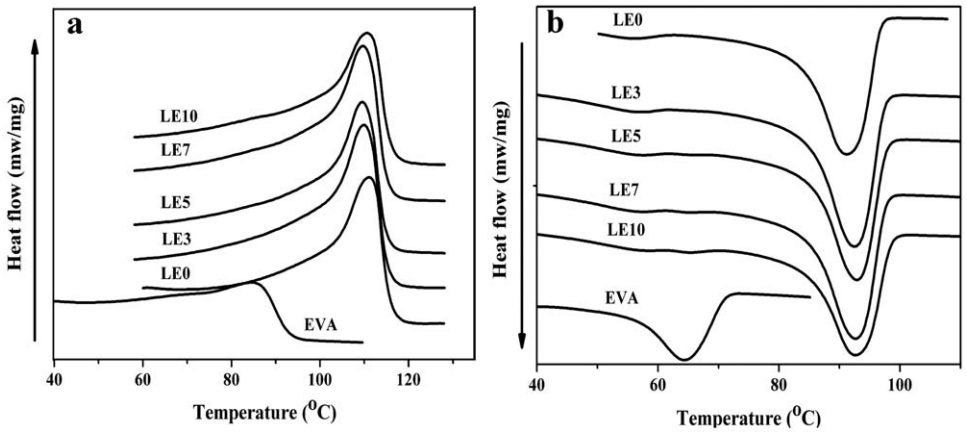

Figure 1. The melting and crystallization curves of LDPE/EVA blends (a: melting, b: crystallization).

1.5 g/10 min, respectively (190°C, 2.16 kg). The HDPE, with trademark DMDA8007, was obtained from Dow Chemical Industry Factory. The LDPE, with the trademark 2210 H, was supplied as pellets by Lanzhou Petrochemical Corp. (Lanzhou, Gansu, China). EVA copolymer grade 462, containing 18% VA, and density of 941 kg/m^3 was obtained from DuPont, American.

Sample Preparation. In this study, HDPE/EVA and LDPE/EVA blends were prepared by melt blending. The melt blends of HDPE/EVA and LDPE/EVA were blended in a mixer (Rheomix 600, Haake, Germany) at 190°C, with the compositions of 100/0, 99/1, 97/3, 95/5, 93/7, and 90/10 wt/wt, which were named LE0, LE1, LE3, LE5, LE7, and LE10 for LDPE/EVA blends separately. The names of HE0, HE1, HE3, HE5, HE7, and HE10 for the HDPE/EVA blends were the same as LDPE/EVA blends. Then the melt blends were compression molded into desired disks at 175°C for measurements. In the preparation of all the blends, the polymers were stabilized by addition of 0.5 wt % antioxidant to prevent thermal-oxidative degradation.

Differential Scanning Calorimetry. The melting behavior of each blend was determined using DSC204 equipment (Netzsch Com., Germany). Experiments were carried out with 6–8 mg of sample under dry nitrogen. All samples were first heated to 165°C at a rate of 10 °C/min, and held at 165°C for 5 min, and then cooled at a rate of 10 °C/min to 20°C and held at 20°C for 3 min. They were then scanned from 20 to 165°C at a rate of 10 °C/min. Crystallization and melting temperatures were obtained from the cooling and the second-heating thermograms, respectively.

Environmental Stress Cracking Resistance Test. This test was performed according to ASTM D1693. Ten notched specimens (38 mm × 13 mm × 2 mm for HDPE/EVA blends and 38 mm × 13 mm × 3 mm for LDPE/EVA blends) were curved into "U" shape and attached to a frame. These samples were then suspended in aqueous 10% Igepal CA-630 solution at 50°C. The time to failure is defined as the time when 50% of the samples are failed during the ESCR test suggested by ASTM D1693.

Dynamic Rheological Measurements. Dynamic rheological measurements were carried out in a Bohlin Geminy 200 stress-controlled rheometer in constant-strain mode. The diameter of the plate was 25 mm, and the gap was about 1 mm. All of the samples were tested in the frequency range from 0.01 to 100 Hz at 180°C, respectively. To keep the response in the linear viscoelastic region, the applied strain was controlled at 1%. The

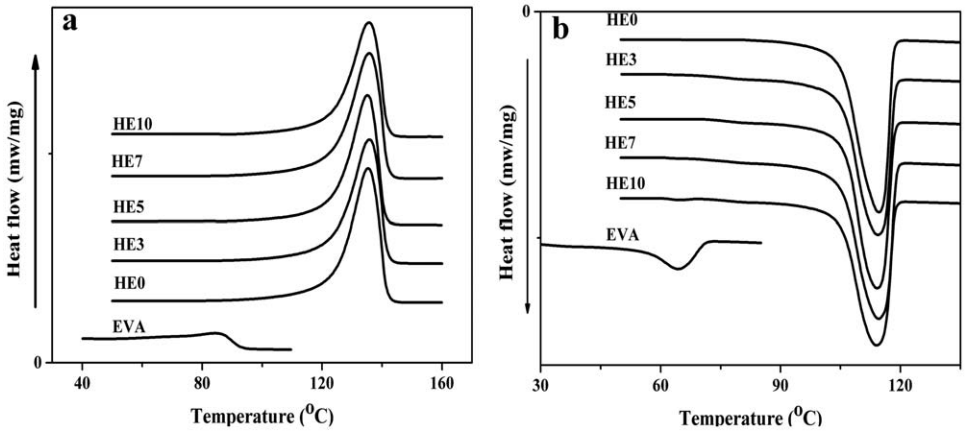

Figure 2. The melting and crystallization curves of HDPE/EVA blends (a: melting, b: crystallization).

Table I. Melting and Crystallization Properties of HDPE/EVA and LDPE/EVA Blends

	HDPE/EVA blends				LDPE/EVA blends			
EVA content (wt %)	Tm[a] (°C)	Tc[b] (°C)	HMW[c] (°C)	Xc[d] (%)	Tm[a] (°C)	Tc[b] (°C)	HMW[c] (°C)	Xc[d] (%)
0	135.4	114.5	10.1	78.3	111.2	91.2	10.4	29.2
3	135.7	114.3	10.2	74.8	110	92.4	12.5	33.5
5	135.2	114.1	10.0	73.2	109.6	92.8	12.9	32.2
7	135.7	114.5	10.4	71.5	109.7	92.6	13.2	31.8
10	135.6	114.1	10.3	69.2	110.3	91.8	13.9	31.2

[a] melting temperature.
[b] crystallization temperature.
[c] half-width of the melting temperature.
[d] crystallinity.

thermal stability of the samples during rheological testing was checked by a time sweep and all of the tests were completed within 10 min.

Mechanical Properties. Tensile testing was determined according to ASTM D638 using an Instron 5562 materials tester. Speed of 100 mm/min was used for the test.

Scanning Electron Microscopy. The samples were cryogenically fractured in liquid nitrogen, and then all the surfaces were gold-coated to enhance image resolution and to avoid electrostatic charging.

After the ESCR test was completed, the failed samples were collected for further analysis of the crack surface by scanning electron microscopy (SEM). Two different sample morphologies were characterized: (1) fracture surface observation by the failed samples to obtain the morphology of the crack surfaces and (2) cross-section view of ESC by microtome sectioning parallel to the crack direction. The morphology of the surfaces was observed by a SEM (JSM-5900LV JOEL, Tokyo, Japan) instrument, using an acceleration voltage of 5 kV.

RESULTS AND DISCUSSION

Thermal Analysis

DSC heating and crystallization curves obtained for LDPE/EVA and HDPE/EVA blends are presented in Figures 1 and 2, respectively. HDPE and LDPE show a single endothermic peak, as well as EVA representative of the melting temperature of their crystallinity. It has been reported that the presence of two peaks for all the PE/EVA blends, except 90/10 wt/wt PE/EVA blend, corresponding to the melting point of different crystalline type, verifies the immiscibility of the PE and EVA crystalline phases.[7] In our study composition range (below 10% wt EVA), a single peak observed for all the blends may verify the co-crystallization in this blend composition with respect to EVA content.

The variation of melting temperature, crystallization temperature, half-width of the melting temperature, and the crystallinity for the two series blends are listed in Table I. For the LDPE/EVA blends, the depression of melting temperature increases in crystallization temperature and crystallinity for LDPE is due to the dilution effect of EVA and/or co-crystallization of LDPE with part of EVA.[7] In addition, the half-width of the melting temperature increase with increasing EVA content, which indicated that part of EVA molecules enter into the crystalline phase of the LDPE. These results show that LDPE/EVA blends are not completely immiscible and there is a partial miscibility between LDPE and EVA in the melt state, which could in turn lead to partial miscibility in the amorphous region in the solid state. On the other hand, partial miscibility in the melt state from one side and also their structural similarity from the other side can lead to their co-crystallization. Thus, there is a high compatibility between LDPE and EVA in this blend composition. However, the half-width of

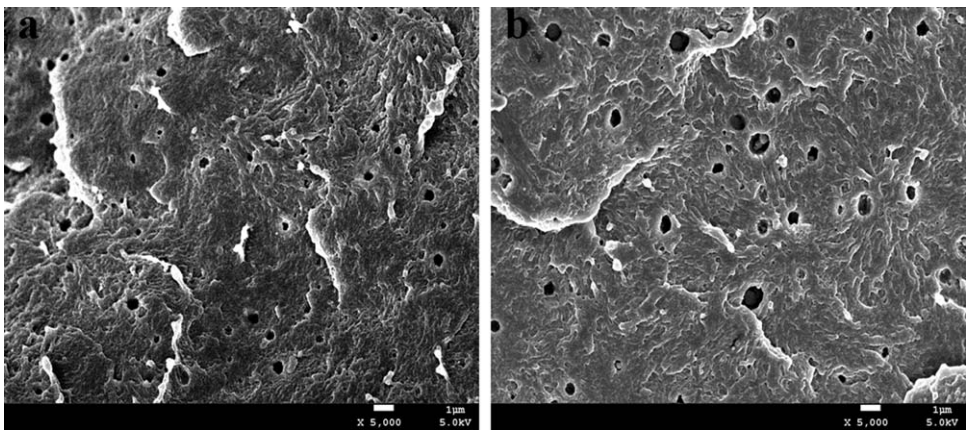

Figure 3. SEM micrographs of the HDPE/EVA blends (a: HE3, b: HE7).

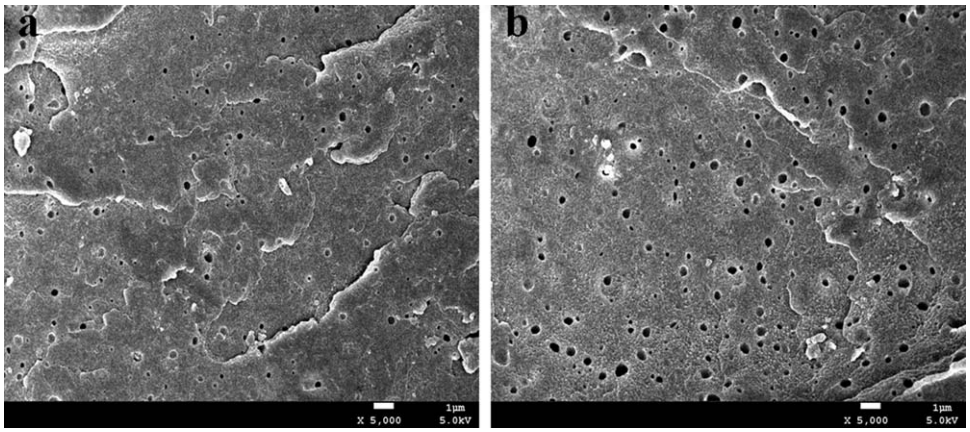

Figure 4. SEM micrographs of the LDPE/EVA blends (a: LE3, b: LE7).

the melting temperature and the melting and crystallization temperature do not change for HDPE/EVA blends suggesting a lower degree of compatibility in this system compared to LDPE/EVA.

Phase Behavior Analysis

SEM micrographs [Figure 3(a,b)] clearly indicate that the HDPE/EVA blends have a two-phase morphology showing the immiscibility of the used HDPE and EVA, in the study composition ranges. Increasing EVA content from 3% to 7% increases the average diameter of the dispersed EVA domains from about 0.38 to 0.61 μm. Figure 4(a,b) shows the obtained SEM micrographs for LDPE/EVA blends. Increasing EVA content from 3% to 7% increases the average diameter of the dispersed EVA domains from about 0.20 to 0.35 μm which is smaller than EVA domains in HDPE/EVA blends. This indicates that the LDPE/EVA blend is more miscible as compared to HDPE/EVA blend for the composition range studied. The better miscibility of LDPE/EVA blends is caused by the similarities between the backbone chains of the LDPE and EVA, both having a branched type structures, whereas HDPE with its linear structure and higher crystallinity is less miscible with the EVA.

To further analyze the phase behavior of the two series blends, we used the Han curves technique developed by Han and Lem[11] in which log G' is plotted versus log G'' and is a useful tool to assess the blend morphological state. For a homogeneous polymer system, the Han curve is independent on the composition and is generally linear. Figure 5 shows the Han curves for LDPE/EVA and HDPE/EVA blends. One can see that the respective G'–G'' curves for LDPE/EVA blends are all linear and show a composition-independent correlation indicating a similar morphological state and high degree of compatibility in the system. This essentially originates from the existence of the structural similarity (microstructure) between blend constituents. However a composition-dependent correlation appears in HDPE/EVA blends suggesting a lower degree of compatibility in this system compared to LDPE/EVA.[9,12,13]

The physical properties of polymer blends are highly affected by the compatibility of the blends. According to brush theory, the inter-diffusion between neighboring polymers resulting in the entanglement of polymer chains is of great importance for bonding between phases.[3] The comparison of the mechanical properties of the two series blends is shown in Figure 6. Since the LDPE/EVA blends show good compatibility compared with the HDPE/EVA blends, thus, with increasing EVA content, the tensile strength increased. While for the HDPE/EVA blends, with increasing EVA content, the tensile strength decreased.

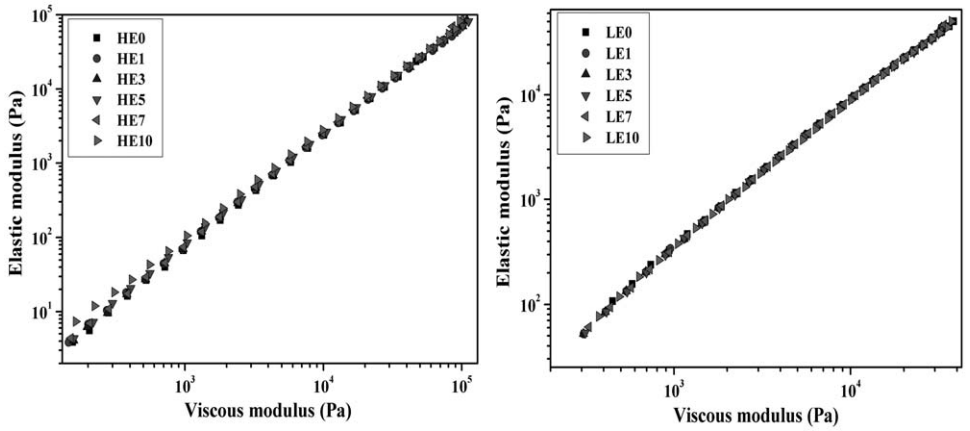

Figure 5. Han curves for HDPE/EVA and LDPE/EVA blends.

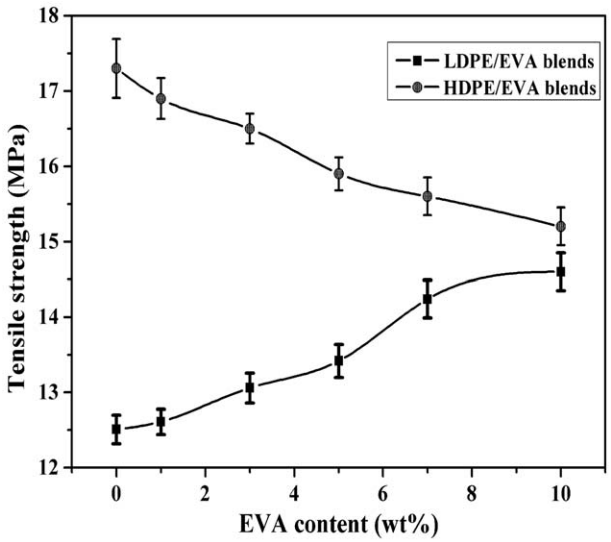

Figure 6. The mechanical properties of the two series blends.

Environmental Stress-Cracking Experiments

The ESCR test was carried out at the temperature of 50°C. The time to failure of different samples are shown in Table II. In most of the cases, cracking starts on both sides in a direction perpendicular to the notch, these small cracks grow and lead to catastrophic failure. However, the LE3, LE5, LE7, and LE10 samples did not fail even for 1000 h. Combined with the above analysis, the reason maybe due to the high impact resistance and high ESCR of EVA phase, as a consequence of which craze initiation and crack growth are likely to be prevented.[6] Although the HDPE/EVA blends show similar phase structure with LDPE/EVA blends, small improvements were observed for HDPE/EVA blends. From the above analysis, a finer and smaller dispersion of the dispersed phase is achieved during mixing for LDPE/EVA blends. Above all, it provides good interfacial adhesion. The inter diffusion between neighboring polymers resulting in the entanglement of polymer chains is of great importance for bonding between phases, and this leads to effective stress transfer between the dispersed phase and the continuous phase, an increase in the interfacial adhesion, and a reduction in the interlayer slip.[3]

Table II. ESCR In Terms of Failure Time of the Various Blend Compositions

Samples	ESCR (h)	Samples	ESCR (h)
HE0	3	LE0	5
HE1	4	LE1	20
HE3	6	LE3	>1000
HE5	8	LE5	>1000
HE7	10	LE7	>1000
HE10	12	LE10	>1000

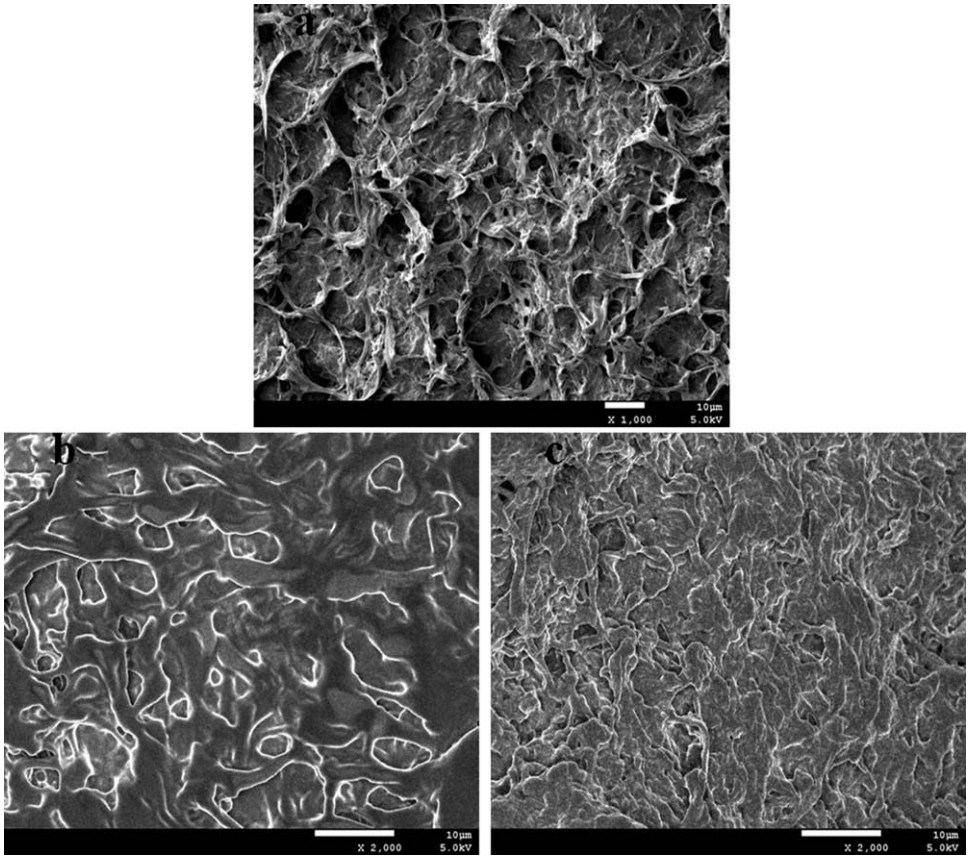

Figure 7. The SEM photos of the crack surfaces of the failed samples. (a: HE0, b: HE3, c: HE7).

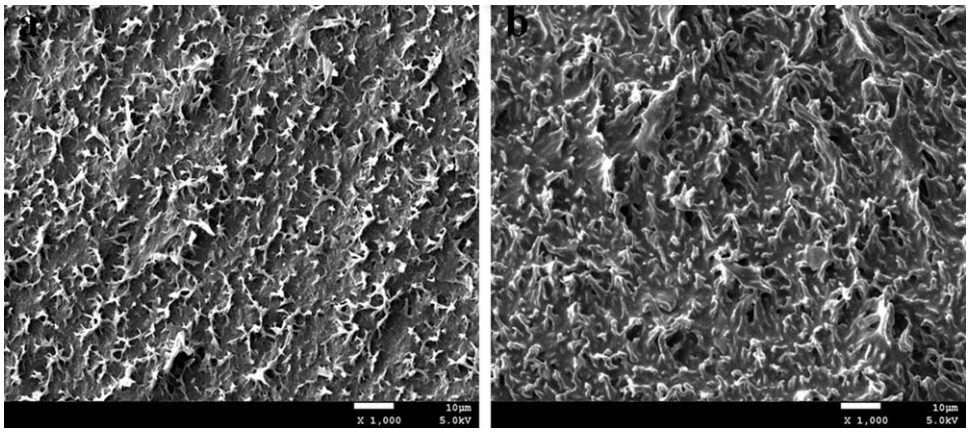

Figure 8. The SEM photos of the crack surfaces of the failed samples. (a: LE0, b: LE1).

Morphology Analysis

It has been reported that the major factor to control ESCR property in the HDPE is the fibrillations, i.e. tie chain density.[14,15] There have been many reports that the creep behavior of process zone, that is, fibrillation within the process zone, can be a determining factor for ESCR properties of HDPE.

Figure 7(a–c) shows the SEM photos of the crack surfaces of HE0, HE3, and HE7. There appears no fibrillation within the crack surface (traces of process zone during crack propagation) for all the HDPE/EVA blends. Figure 8(a,b) shows the SEM photos of the crack surfaces of LE0 and LE1, respectively. With increasing EVA content, the size of fibrillation became large. The fibrils with high resistance to an aggressive environment can act as a "tie" in the crack tip, leading to a decrease in the rate of crack propagation.[10] Since all the other LDPE/EVA blends did not fail in the test, thus we did not study the crack surfaces of them. Furthermore, the cross-section view of ESC by microtome sectioning parallel to the crack direction was analyzed.

Figure 9 is a high magnification picture of the region parallel to the crack direction at different hours (1 h, 6 h) for the sample HE3. In Figure 8(a), voids are seen, presumably caused by the Igepal. But after 6 h, the internally large voids have advanced significantly through crazing and cracking which cause failure in the ESCR. Figure 10 is a high magnification picture of the region parallel to the crack direction at different hours (10 h, 1000 h) for the sample LE3. Under external stress, stress concentration gives rise to cracking and formation of micro-voids inside the blend. The result is a higher local stress concentration between the particles. In the figures, voids are seen to have been formed but the material has not been drawn enough to cause failure.

In the case of LDPE/EVA blends, there are many fine and well adhered EVA particles in the PE matrix. Therefore, overlapping of stress fields caused by neighboring particles in LDPE/EVA blends is more predominant than in HDPE/EVA blends because there are more and closer stress concentration points. This could induce more toughening mechanisms in deformation zones and intensify the plastic work, and possibly enable particles to cavitate and create a stress state beneficial for initiation of shear bands in addition to crazing,[6] which is the main toughening mechanism of LDPE/EVA. As discussed before, and supported by SEM analysis, in the fracture process of LDPE/EVA blends, due to the presence of strong interface between the EVA and the matrix phase, more fibrils with high resistance to an aggressive environment can act as a "tie" in the crack tip appears.[10] These types of deformation cause the consumption of more energy in the fracture process, leading to the highest ESCR for LDPE/EVA blends. The failure mechanism of the two series blends are shown in Figure 11.

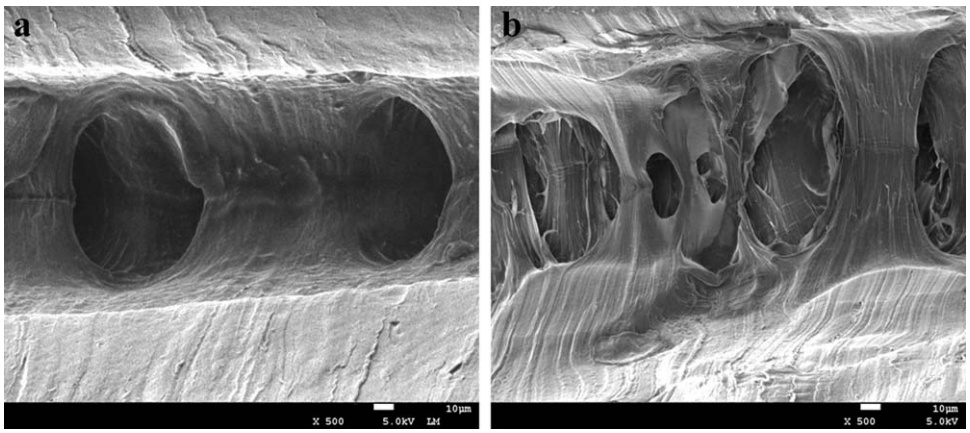

Figure 9. The SEM photos of the region parallel to the crack direction at different hours (a: 1 h, b: 5 h,) for the sample HE3.

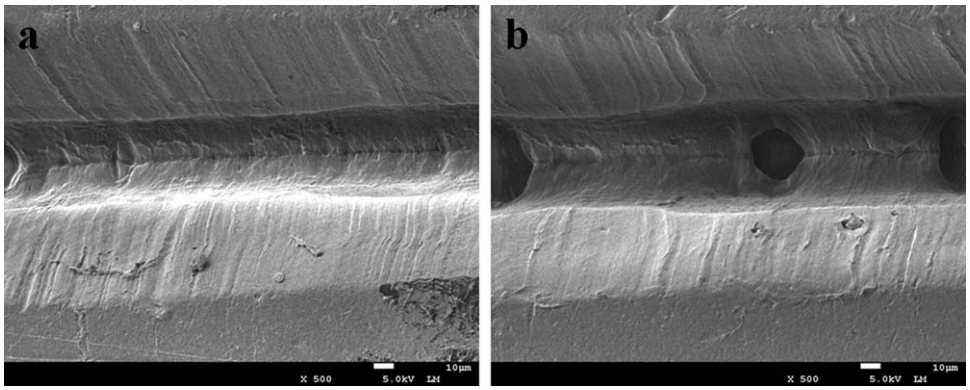

Figure 10. The SEM photos of the region parallel to the crack direction at different hours (a:10 h, b:1000 h,) for the sample LE3.

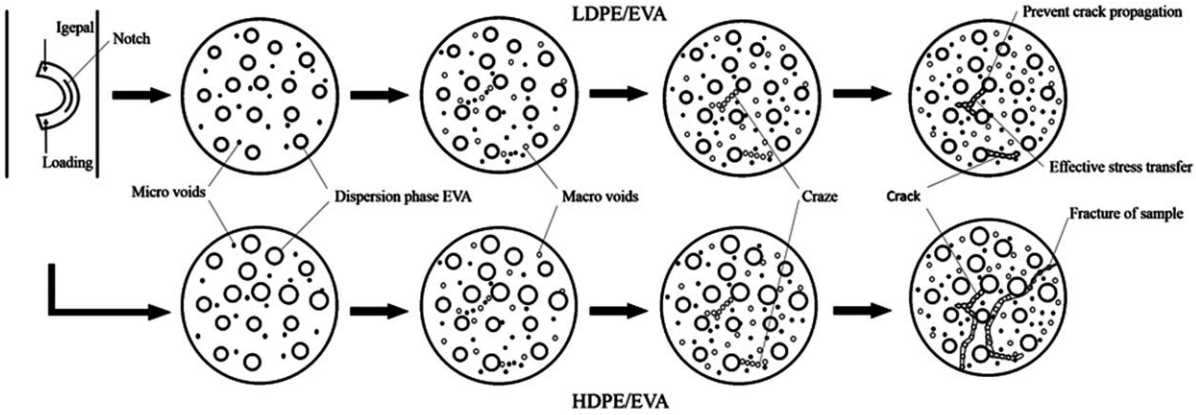

Figure 11. The failure mechanism of the two series blends.

CONCLUSIONS

In this study, the ESCR performance of HDPE/EVA and LDPE/EVA blends was determined. The analysis showed that the detachment of the EVA phase from the PE matrix is probably due to the influence of the ESCR. Under external stress, stress concentration gives rise to cracking and formation of microvoids inside the blend. The result is a higher local stress concentration between the particles. There is an effect influencing crack propagation. Cracks, which enter the elongated microvoids, are rounded at their tips. These cracks are prevented from further propagation.[6,16]

Although the HDPE/EVA blends show similar phase structure with LDPE/EVA blends, the small improvements were observed for HDPE/EVA blends. From the phase behavior analysis, a finer and smaller dispersion of the dispersed phase is achieved during mixing for LDPE/EVA blends. Above all, it provides good interfacial adhesion. The inter diffusion between neighboring polymers resulting in the entanglement of polymer chains is of great importance for bonding between phases, and this leads to effective stress transfer between the dispersed phase and the continuous phase, an increase in the interfacial adhesion, and a reduction in the interlayer slip. This could induce more fibrils with high resistance to an aggressive environment and can act as a "tie" in the crack tip appears. These types of deformation cause the consumption of more energy in the fracture process, leading to the highest ESCR for LDPE/EVA blends.

ACKNOWLEDGMENTS

The authors would like to thank National Natural Science Foundation of China (50903049, 51273118) and Provincial Science and Technology Pillar Program of Sichuan (2013FZ0006, China), for financial support, and thank Analytical and Testing Center of Sichuan University for providing measurements.

REFERENCES

1. Munaro, M.; Akcelrud, L. *Polym. Degrad. Stab.* **2008**, *93*, 43.
2. Whiteley, K. S.; Heggs, T. G.; Koch, H.; Mawer, R. L.; Immel, W. *Ullmann's Encyclopedia of Industrial Chemistry VCH* **1992**, *21*, 494.
3. Moly, K. A.; Bhagawan, S. S.; Groeninckx, G.; Thomas, S. *J. Appl. Polym. Sci.* **2006**, *100*, 4526.
4. Datta, S. K.; Bhowmick, A. K.; Mukunda, P. G.; Chaki, T. K. *Polym. Degrad. Stab.* **1995**, *50*, 75.
5. Oshima, A.; Ikeda, S.; Seguchi, T.; Tabata, Y. *Radiat. Phys. Chem.* **1997**, *49*, 279.
6. Borsova, B.; Kressler, J. *Macromol. Mater. Eng.* **2003**, *288*, 509.

7. Faker, M.; Razavi Aghjeh, M. K.; Ghaffari, M.; Seyyedi, S. A. *Eur. Polym. J.* **2008**, *44*, 1834.
8. Ward, A. L.; Lu, X.; Huang, Y.; Brown, N. *Polymer* **1991**, *32*, 2172.
9. Khonakdar, H. A.; Jafari, S. H.; Yavari, A.; Asadinezhad, A.; Wagenknecht, U. *Polym. Bull.* **2005**, *54*, 7.
10. Khodabandelou, M.; Razavi Aghjeh, M. K.; Rezaei, M. *Eng. Fract. Mech.* **2009**, *76*, 2856.
11. Han, C. D.; Lem, K. W. *Polym. Eng. Rev.* **1983**, *12*, 135.
12. Wu, T.; Li, Y.; Zhang, D. L.; Liao, S. Q.; Tan, H. M. *J. Appl. Polym. Sci.* **2004**, *91*, 905.
13. Takidis, G.; Bikiaris, D. N.; Papa Georgiou, G. Z.; Achilias, D. S.; Sideridou, I. *J. Appl. Polym. Sci.* **2003**, *90*, 841.
14. Rose, L. J.; Channell, A. D.; Frye, C. L.; Capaccio, G. *J. Appl. Polym. Sci.* **1994**, *54*, 2119.
15. Barry, D. B.; Delatycki, O. *Polymer* **1992**, *33*, 1261.
16. Moyses, S. G. *Polym. J.* **2000**, *32*, 486.